

## Experimental and theoretical study of the electronic structure of Fe, Co, and Ni aluminides with the $B2$ structure

G. A. Botton

*Department of Materials Science and Metallurgy, University of Cambridge, Pembroke Street, Cambridge, CB2 3QZ, United Kingdom*

G. Y. Guo and W. M. Temmerman

*Daresbury Laboratory, Warrington, WA4 4AD, United Kingdom*

C. J. Humphreys

*Department of Materials Science and Metallurgy, University of Cambridge, Pembroke Street, Cambridge, CB2 3QZ, United Kingdom*

(Received 6 February 1996)

The differences in electronic structure of  $B2$ -type (CsCl) transition-metal aluminides (FeAl, CoAl, and NiAl) have been investigated by comparing data obtained using electron energy-loss spectroscopy with theoretical calculations of the spectra. The densities of states (DOS) for the three alloys calculated using the *ab initio* self-consistent linear muffin-tin orbital method within the local density approximation have been compared. Using the unoccupied part of the DOS and the relevant transition matrix elements, energy-loss spectra have been calculated. It is noted that a rigid band model can only be considered as a first approximation to calculate the trends in the electronic structure of the alloys. The Al  $L_{2-3}$  and  $K$  edges (providing information on  $s+d$  and  $p$  symmetry of final states at the Al sites, respectively) and the transition-metal  $L_{2-3}$  edges ( $s+d$  symmetry of final states at the transition-metal sites) have been studied. Good agreement has been found between experiment and calculations and, from the interpretation of spectral details in terms of site and angular momentum decomposed density of states, hybridization and interaction between the Al  $sp$  and TM  $d$  bands is observed and thus a covalent character in the bond is concluded. The differences in the electronic structure of the alloys studied, both in terms of band filling and density of states at the Fermi level, have been correlated with the variation of the macroscopic properties of the materials. [S0163-1829(96)09827-X]

### I. INTRODUCTION

Transition-metal (TM) aluminides are of considerable technological interest for high-temperature applications. A particular system that has recently received great attention is the series of neighboring element TM aluminides FeAl, CoAl, and NiAl. As these materials have the same CsCl ( $B2$ ) crystallographic structure, but exhibit different mechanical and magnetic properties, they constitute an ideal test case to study systematic variations in the electronic structure, which can potentially be related to the variations of macroscopic mechanical or magnetic properties. As a first step towards the ultimate goal of understanding macroscopic properties, it is important to improve our understanding of experimental data directly related to the electronic structure, as provided by spectroscopic techniques, in order to retrieve useful bonding information and assess the precision of the various *ab initio* techniques used to model the spectral features. In this paper we present, therefore, a comparison of experimental data obtained by electron energy-loss spectroscopy (EELS) and calculated spectra based on first-principles (*ab initio*) electronic structure calculations. We discuss the origin of the spectral features in terms of the density of initial and final states, the angular momentum character of these states, and, from the experiment-theory comparison, we address trends in the electronic structure in the series, the bonding character in these aluminides, and finally the validity of the application of a simplified rigid band model to this system.

The variation in bonding character in this particular series has been recently investigated from a theoretical point of view by Schultz and Davenport<sup>1</sup> who attempted to correlate their results with the mechanical behavior and by Zou and Fu<sup>2</sup> who discussed the trends in the entire row of  $3d$  TM aluminides (from early TM to late TM). In a detailed analysis, Gelatt, Williams, and Moruzzi<sup>3</sup> have discussed the general theory of TM–non-TM bonding and showed the trends in the heat of formation as a function of the number of  $d$  electrons. Although showing good agreement with experimental heats of formation and the empirical Miedema's treatment, no comparison with experimental spectroscopies has been made in this theoretical work.

Earlier experimental work was carried out on this series by Wenger, Bürri, and Steinemann<sup>4</sup> and Kapoor *et al.*<sup>5</sup> using soft x-ray emission. By comparing the integrated and normalized intensity of the emission spectra Wenger, Bürri, and Steinemann addressed the question of charge transfer. In their work, however, the spectral distributions were not presented and the hybridization of the TM and Al bands was not considered as a possible contribution to their observations. Detailed information on the Al spectral distributions was obtained by Kapoor *et al.*<sup>5</sup> but the analysis did not include important complementary data on the TM states. Fuggle *et al.*,<sup>6</sup> from valence band spectroscopy, showed a filling of the Ni  $d$  bands in NiAl and realized the importance of obtaining complementary information from unoccupied states in order to confirm the band filling conclusions.

This complementary information to early results can be

obtained by electron energy-loss spectroscopy, which provides information on both occupied and unoccupied electronic states and is thus equivalent to x-ray absorption spectroscopy (XAS). The technique is extremely sensitive to changes in chemical environment and recent comparison of experiments with theory shows that a wealth of information can be obtained on the local electronic structure of materials.<sup>7</sup> The advantage of EELS over XAS or methods dealing only with occupied states, however, resides on the fact that information can be obtained at very high spatial resolution down to the nanometer or subnanometer level<sup>8</sup> and therefore detailed information about the local electronic structure at defects can be sought potentially. A full understanding of the spectroscopic data from the relatively perfect material is, however, essential prior to the analysis of defects in crystals.

The electronic structure calculations we use in this work are performed using the linear muffin-tin orbital (LMTO) technique as the method has been successful in the study of the stability of aluminides (e.g., Nicholson *et al.*,<sup>9</sup> Barbieri *et al.*,<sup>10</sup> Nguyen Mahn, Bratkovsky, and Pettifor<sup>11</sup>). Experimental results for the TM  $L_{2,3}$  edge and Al  $K$  and  $L_{2,3}$  edges show systematic variations in the near-edge structure and an agreement with calculated spectra. From the density of states (DOS) in the series we conclude that a rigid band can be used only as a first approximation to study the trends in this series. We show that there is an Al  $p$ -TM  $d$  hybridization contribution, and that bonding introduces  $d$  character at the Al site.

In Sec. II we describe the theoretical framework used to calculate the spectra and the experimental methods to obtain EELS near-edge structure data. In Sec. III we present the experimental results, the calculated DOS and spectra, and finally we discuss, in Sec. IV, the trends in the electronic structure of the alloys both in terms of the changes in spectroscopic data and in terms of the macroscopic properties.

## II. METHODS

### A. Theoretical methods

The analysis of the near-edge structure (NES) in electron energy-loss spectroscopy allows the site-dependent electronic structure to be probed as the spectrum arises from transitions from core levels to the first unoccupied states above the Fermi level. The probability ( $\Omega$ ) of a transition from a level of angular momentum  $L$  to final states with angular momenta  $L+1$  and  $L-1$  will be, as derived from Fermi's golden rule,<sup>12</sup> proportional to

$$\Omega_L \propto \{|M_{L+1}|^2 \rho_{L+1} + |M_{L-1}|^2 \rho_{L-1}\}, \quad (1)$$

where  $M_{L\pm 1}$  is the matrix element for the transition to a final state of angular momentum  $L\pm 1$  and  $\rho_{L\pm 1}$  is the density of unoccupied states above the Fermi level resolved in their angular momentum components. The matrix elements  $M_{L\pm 1}$  are given by

$$M_{L\pm 1} = \int d\mathbf{r} \psi_L^*(\mathbf{r}) \mathcal{H} \psi_{L\pm 1}(\mathbf{r}) \quad (2)$$

and are related to the overlap of initial- and final-state wave functions  $\psi_L$  and  $\psi_{L\pm 1}$  and  $\mathcal{H}$  represents the electron-

electron interaction (see Vvedensky<sup>13</sup> for details). For inner-shell excitations the density of initial states  $\rho_L$  is considered as a  $\delta$  function and thus spin-orbit coupled  $2p_{3/2}$  and  $2p_{1/2}$  initial states will generate two distinct sets of peaks each one being combined through Eq. (1) to give rise to the  $L_{2,3}$  edge. This theoretical treatment is equivalent to the one used in x-ray absorption spectroscopy for small scattering angles where the dipole approximation is valid. Nondipole allowed transitions in EELS can be neglected in the NES region as they have been shown to contribute only at energies significantly higher than the edge threshold.<sup>14</sup> From Eq. (1), the EELS near-edge structure contains information on the density of unoccupied states. For nonzero matrix elements in Eq. (1) there must be an overlap between the initial- and final-state wave functions for a transition to occur, thus the DOS must be local within the atomic sphere for a particular atom and the DOS may be decomposed into angular momenta of  $s$ ,  $p$ , and  $d$  character using the  $\Delta l = \pm 1$  selection rule. For initial  $1s$  levels, transitions will occur into  $p$  symmetry final states whereas for initial  $2p$  levels the transitions will be into  $s$  and  $d$  symmetry final states. Calculations of the DOS have been carried out with a self-consistent LMTO method using the atomic-sphere approximation (ASA).<sup>15-17</sup> The calculations are based on density functional theory with the local density approximation (LDA). The standard local exchange-correlation potential of von Barth and Hedin<sup>18</sup> is used. The LMTO-ASA method assumes spherically symmetric potentials inside overlapping spheres and a combined correction was used to account for sphere overlap. Valence basis functions ( $s, p, d$ ) for Al and TM atoms were used. The density of states was obtained with the tetrahedron method of integration using 89  $k$  points as described by Poumellec, Durham, and Guo<sup>19</sup> and spectra are successively broadened with a Lorentzian distribution to account for lifetime and experimental resolution. Difficulties in the comparison of experiment and theory using Eq. (1) arise from many-body effects under the influence of the core hole caused by the transition for  $L_{2,3}$  edges  $2p^6 3d^n \rightarrow 2p^5 3d^{n+1}$  causing an intensity redistribution such that the white lines cannot be directly interpreted as the exact DOS distribution because of the Coulomb hole and exchange interactions. Such effects have been discussed by Zaanen *et al.*<sup>20</sup> and Fink *et al.*<sup>21</sup> who commented, however, on the fact that Coulomb hole and exchange interaction effects should be reduced if screening is effective. The validity of our calculations without the inclusion of these many-body effects will be analyzed in the discussion section. Although the exact modeling of the fine structure is quite complex, very useful information can be simply obtained about  $d$ -band occupancy as described by Pearson, Ahn, and Fultz<sup>14</sup> who correlated the intensity of the  $3d$  and  $4d$  TM white lines, as normalized to the continuum after the edge, to the  $d$ -band hole count.

### B. Experimental method

Samples were prepared by arc melting materials of high purity (99.98% for Fe, Co, and Ni and 99.999% for Al) followed by homogenization in an Ar atmosphere at a tem-

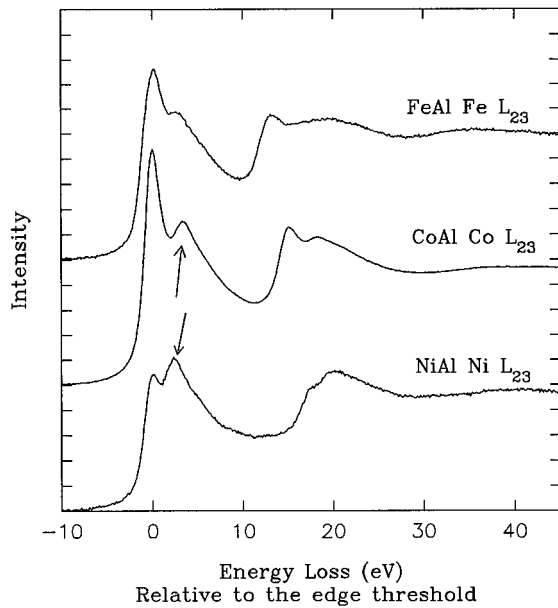


FIG. 1. Transition metal  $L_{2-3}$  edges in FeAl, CoAl, and NiAl. The intensity scale is constant for the three spectra, which have been only displaced vertically for clarity. The arrow points to the shoulder of the white line as referenced in the text.

perature of about 80% of the melting point and then by slow cooling. Thin specimens were prepared by electropolishing, and energy-loss measurements were carried out soon after thin foil preparation to minimize any possible oxidation effects.

The energy-loss experiments were carried out on a Philips CM30 electron microscope equipped with a parallel detection electron energy-loss spectrometer (Gatan 666 model). In order to increase the energy-loss spectrum resolution, the microscope operating voltage used was 100 kV and the  $\text{LaB}_6$  filament was operated under saturation. In these conditions, spectra with an energy resolution (measured by the full width at half maximum of source profile) of 1.1 eV or better for 30 s acquisition can be obtained. Spectra from areas of similar thickness, as measured relative to the total inelastic mean free path of the 100-keV electrons, were compared so that the effects of multiple inelastic scattering are comparable in all the spectra. For the Al  $L_{2-3}$  edges, spectra were also deconvoluted using the Fourier-log method as the low-loss contribution was included in the same spectrum.

Spectra were corrected for the detector channel-to-channel gain variations by acquiring several spectra (about 7–10) at different positions on the photodiode array and averaging them to produce a gain corrected spectrum as described by Boothroyd, Sato, and Yamada.<sup>22</sup> The continuum background was subtracted using a power-law standard procedure.<sup>23</sup> In NiAl, due to the overlap of the Ni  $M_{2-3}$  (68 eV) and the Al  $L_{2-3}$  edges ( $\sim 73$  eV), a reliable extrapolation of the pre-Al  $L_{2-3}$  background could not be carried out. Analyses with energy dispersive x-ray spectroscopy on the same foils as EELS was carried out revealed that the composition of the alloys was to within 0.2% of the nominal stoichiometric composition.

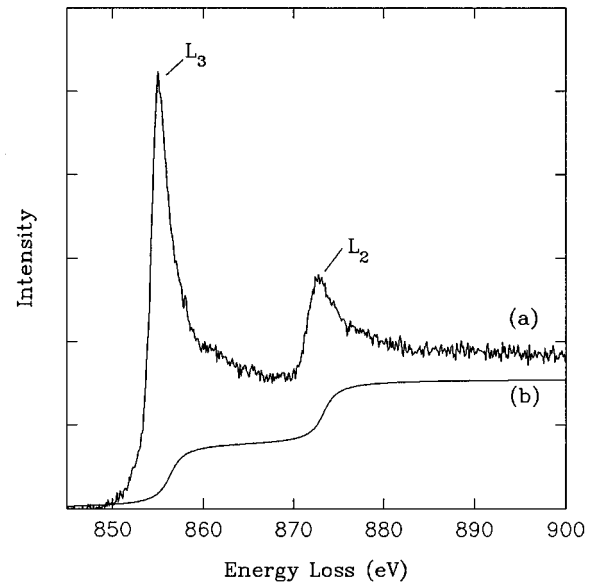


FIG. 2. Ni  $L_{2-3}$  edge in pure Ni (curve *a*) and continuum background under the white line (curve *b*).

### III. RESULTS

#### A. Experimental spectra

##### 1. TM $L_{2-3}$ edges

The transition-metal white-line intensities from alloys (Fig. 1) [when normalized with respect to the continuum background after the edge threshold, so that the white-line signal from the same number of atoms (in the pure elements and in the alloy) is effectively compared<sup>14</sup>] are dramatically reduced compared with the pure metal  $L$  edges presented in the literature (see, for example, Leapman, Grunes, and Fejes<sup>24</sup> and Fink *et al.*<sup>21</sup>). Qualitatively this effect is shown in our experiments and is demonstrated here in the case of the Ni  $L_{23}$  edge in pure Ni (Fig. 2) for a specimen of comparable thickness to the NiAl in Fig. 1 and indicates that upon alloying the  $d$  bands are increasingly occupied, hence the density of unoccupied states is reduced and thus the  $L_{2-3}$  white-line intensity is reduced. A similar effect, particularly evident in NiAl, is observed for the  $M$  edges as described in the following section. Further to this reduced white-line intensity, the evolution of a secondary peak, which appears as a shoulder in the FeAl Fe  $L_3$  white line (not detected in the pure TM) into a well resolved peak can be observed when we progress towards NiAl (Fig. 1). We note also that the white lines are weakest in the NiAl spectrum (Fig. 1), which indicates that the number of unoccupied  $d$  states is lowest in NiAl.

##### 2. Al $L_{23}$ and $K$ edges

Important changes are observed at the Al sites where the intensity distribution is considerably altered relative to the Al  $L_{2-3}$  edge in pure Al [Fig. 3(a)]. Compared with pure Al, there is higher intensity at the threshold (a shoulder relative to the main edge) and a well resolved peak. Because of the overlap with the Ni  $M$  edge (which is also much smaller than in pure Ni and features a weak double-peak structure) [Fig. 3(b)], the Al  $L_{2-3}$  edge in NiAl could not be extracted reli-

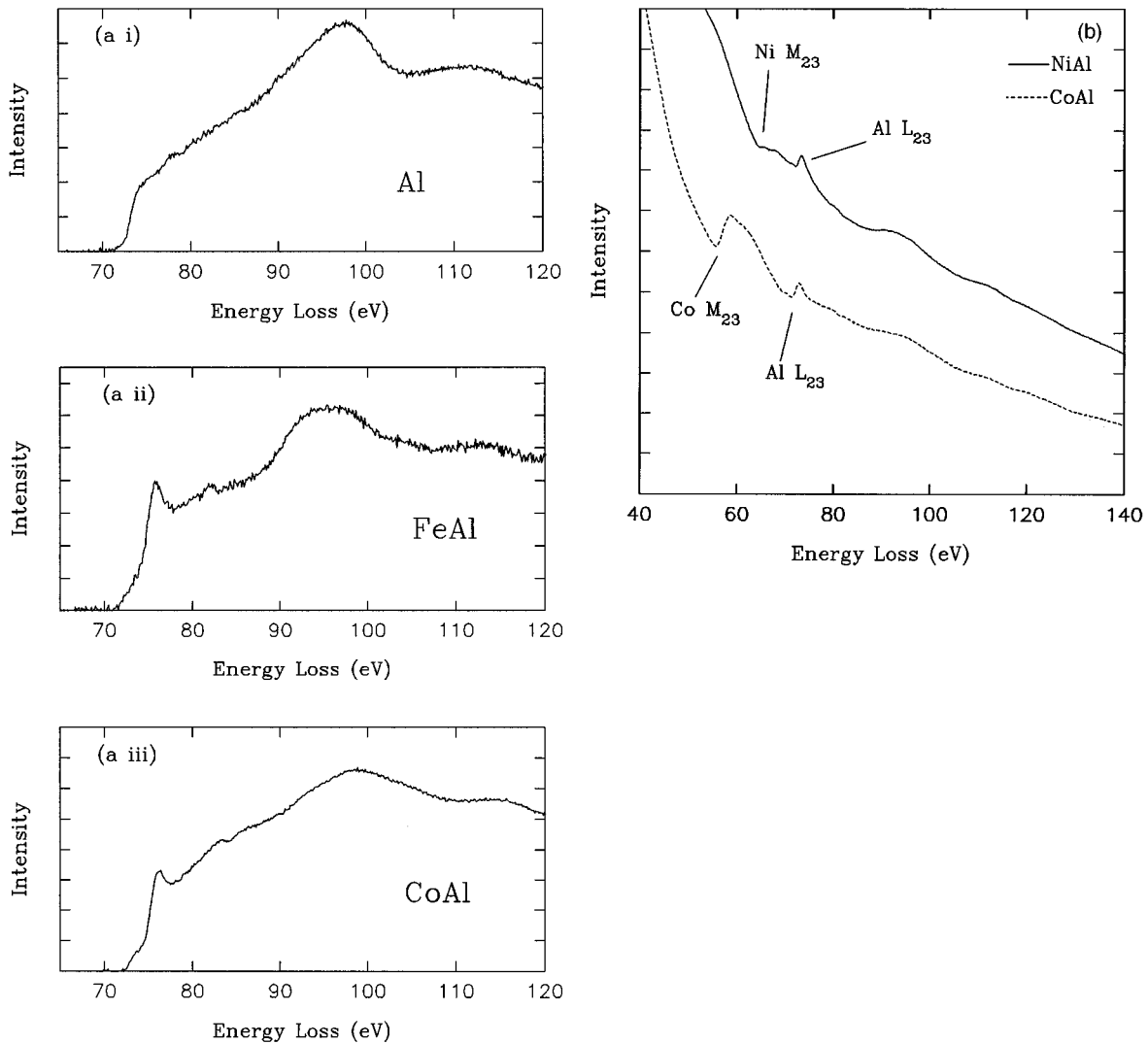


FIG. 3. (a) Al  $L_{2,3}$  edges in (i) pure Al, (ii) FeAl, and (iii) CoAl. Because of edge overlap, the Al  $L_{2,3}$  edge in NiAl could not be subtracted. (b) Energy-loss spectra showing the Al  $L_{2,3}$  and transition-metal  $M_{2,3}$  edges in CoAl and NiAl. The edges have been shifted vertically on the intensity scale.

ably, but from the direct spectrum without background subtraction [Fig. 3(b)], it is clear that the intensity change in the NiAl Al  $L_{2,3}$  edge is qualitatively comparable to the one observed in CoAl. In comparison to pure Al, we also observe an important redistribution of the  $K$  edge intensity near the threshold in the alloy (Fig. 4) as a prepeak is present. The intensity of the prepeak is the weakest for NiAl (a shoulder at the edge being barely visible) and strongest in FeAl and CoAl.

### B. Theoretical calculations and comparison with experiments

As a preliminary comparison of the electronic structure in the series, we analyze important features of the calculated DOS. The total DOS distributions in the three TM aluminides (Fig. 5) are strongly similar and this effect is being taken to suggest that a rigid band model can be used as a first approximation to study the changes in the structure of the three aluminides when neighboring TM are changed. This effect has been concluded previously for the same alloys<sup>25</sup> (although not when doped<sup>26</sup>) and has also been pointed out

by Gellat, Williams, and Moruzzi<sup>3</sup> in the more general case of TM to non-TM bonding when the non-TM is not changed. A more detailed analysis, however, shows that a rigid band model is not adequate as the widths of the valence band (a parameter related to the heat of formation and correlated to the lattice constants and the cohesive properties of a material<sup>27</sup>) are different in the three alloys and thus the Fermi energy ( $E_F$ ) variation does not simply correspond to a decrease of one valence electron in the NiAl DOS upon going from NiAl to CoAl and from CoAl to FeAl. Using the NiAl DOS as a reference band, our calculations show that  $E_F$  in CoAl is 0.08 Ry lower than that in NiAl (instead of 0.05 Ry using a rigid band) and  $E_F$  in FeAl is 0.13 Ry lower than that in NiAl (instead of 0.105 Ry using a rigid band). These values will be compared to our experimental results in Sec. IV.

The DOS profiles of CoAl and NiAl (Fig. 5) agree with previous calculations using other computational techniques such as augmented spherical waves<sup>28</sup> (ASW) and full-potential linear augmented plane wave (FLAPW).<sup>2,29</sup> The main features of the total DOS are assigned, with increasing

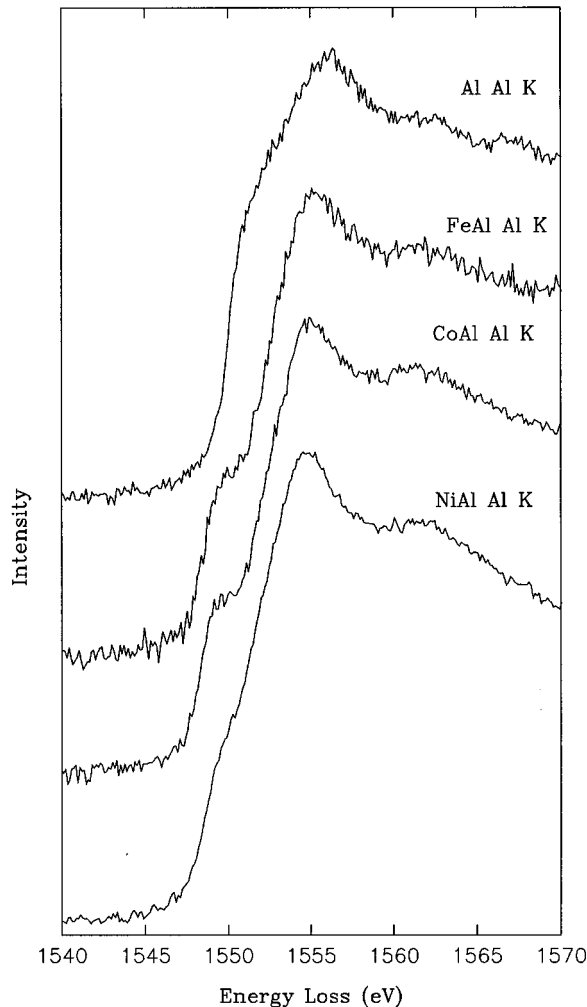


FIG. 4. Al  $K$  edges in pure Al and in the transition-metal aluminides.

energy, by Gelatt, Williams, and Moruzzi<sup>3</sup> and Zou and Fu<sup>2</sup> as the bonding, nonbonding (the peak just below  $E_F$  in NiAl), and antibonding states. A “pseudogap” separating the bonding and nonbonding is well defined in our DOS. Thus from Fig. 5, the position of the  $E_F$  is in the nonbonding states for CoAl, approaching the antibonding states in NiAl and in the bonding states in FeAl. A decomposition of the total DOS into the TM and Al sites also reveals [Figs. 5(a) and 5(b)] that the DOS is dominated, not unexpectedly, by the TM features. Although Gelatt, Williams, and Moruzzi,<sup>3</sup> and Zou and Fu<sup>2</sup> have assigned a nonbonding character to the peak at  $E_F$  in CoAl, our analysis shows that there is some nonnegligible Al  $p$  amplitude, in agreement with Freeman *et al.*,<sup>29</sup> when this amplitude is compared with the maxima in the  $p$  character DOS at the Al sites in the bonding bands with the TM  $d$  bands. From symmetry arguments, however, the  $d$  bands do not have the correct symmetry to form bonding hybrids with the Al  $p$  bands in the “nonbonding” energy range (from FLAPW charge distributions, Zou and Fu<sup>2</sup> have thus assigned an  $e_g$  symmetry to this band). We see also that the amplitude of the antibonding hybrids are concentrated on the Al sites whereas the bonding hybrids have larger amplitude on the TM sites. From such a distribution Gelatt, Williams, and Moruzzi<sup>3</sup> have suggested that, as more bonding

states than antibonding states are filled, charge transfer from the atom with less tightly bound orbitals (Al) to the atoms with more tightly bound orbitals should be expected.

Using the angular momentum decomposed DOS, with  $E_F$  positioned as shown in Fig. 5, and the matrix elements accounted for as described above, the TM  $L_{23}$  spectra have been calculated (Fig. 6). Once the atomic transitions to higher energy continuum states are accounted for using a step function as proposed by Stöhr<sup>30</sup> (as shown in Fig. 2, curve *b*), the agreement between experiment and theory is excellent for the TM  $L_{23}$  edges of Ni, Co, and Fe reproducing the double-peak structure and energy separation. The fact that the continuum is not directly reproduced will be discussed in the following section. Calculated spectra are shown using the same intensity scale (the same units) so that the white-line intensities can be compared from one alloy to the other. The changes in relative intensity in the white-line series show excellent agreement with our data for NiAl and CoAl (the intensity of the Co  $L$  white line being twice the intensity of the Ni  $L$ ) whereas the relative change between Co  $L$  and Fe  $L$  is slightly overestimated in the calculations, though the trend is again reproduced (the intensities of the two white lines are comparable).

A comparison of the calculated (Fig. 7) and experimental [Fig. 3(a)] Al  $L_{23}$  edges for FeAl and CoAl (Fig. 7) also indicates good agreement with the experimental data in showing the increased intensity near the threshold and the well-resolved peak at about 5 eV after the threshold. The sharp peak at about 10 eV above the threshold did not agree with the experimental spectra although a well-defined feature is present at that energy for both experimental FeAl and CoAl spectra. A significant comparison between the experimental and calculated spectra for NiAl could not be carried out due to the overlap described above. We note, however, that in the calculated spectrum the intensity at the threshold is not as strong as in the experimental CoAl and FeAl spectra. The attempts to calculate the Al  $K$  edges are also reasonably successful (Fig. 8, compare with Fig. 4). The presence of a well-resolved shoulder of similar intensity for the FeAl and CoAl, which is less developed (but still present) in the NiAl spectrum, is well reproduced. Relative to the maxima of the edge, the intensity of the shoulder is also reproduced. The secondary peak at 10 eV above the threshold, however, is not clearly present in the experimental spectra. We note qualitatively that the increase in intensity of the edge with respect to pure Al arises, as indicated by the DOS, from an increased empty  $p$  character at the Al site. We note that this effect is still present in NiAl although less pronounced.

#### IV. DISCUSSION

The general agreement between experiments and theory is remarkable considering that we are probing unoccupied states and we are interpreting the spectra with a single-particle DOS without proper consideration of the excitation spectrum. This agreement may arise from the fact that the  $d$  bands are almost full and are therefore quite successful in screening the unoccupied bands from the core hole so that an

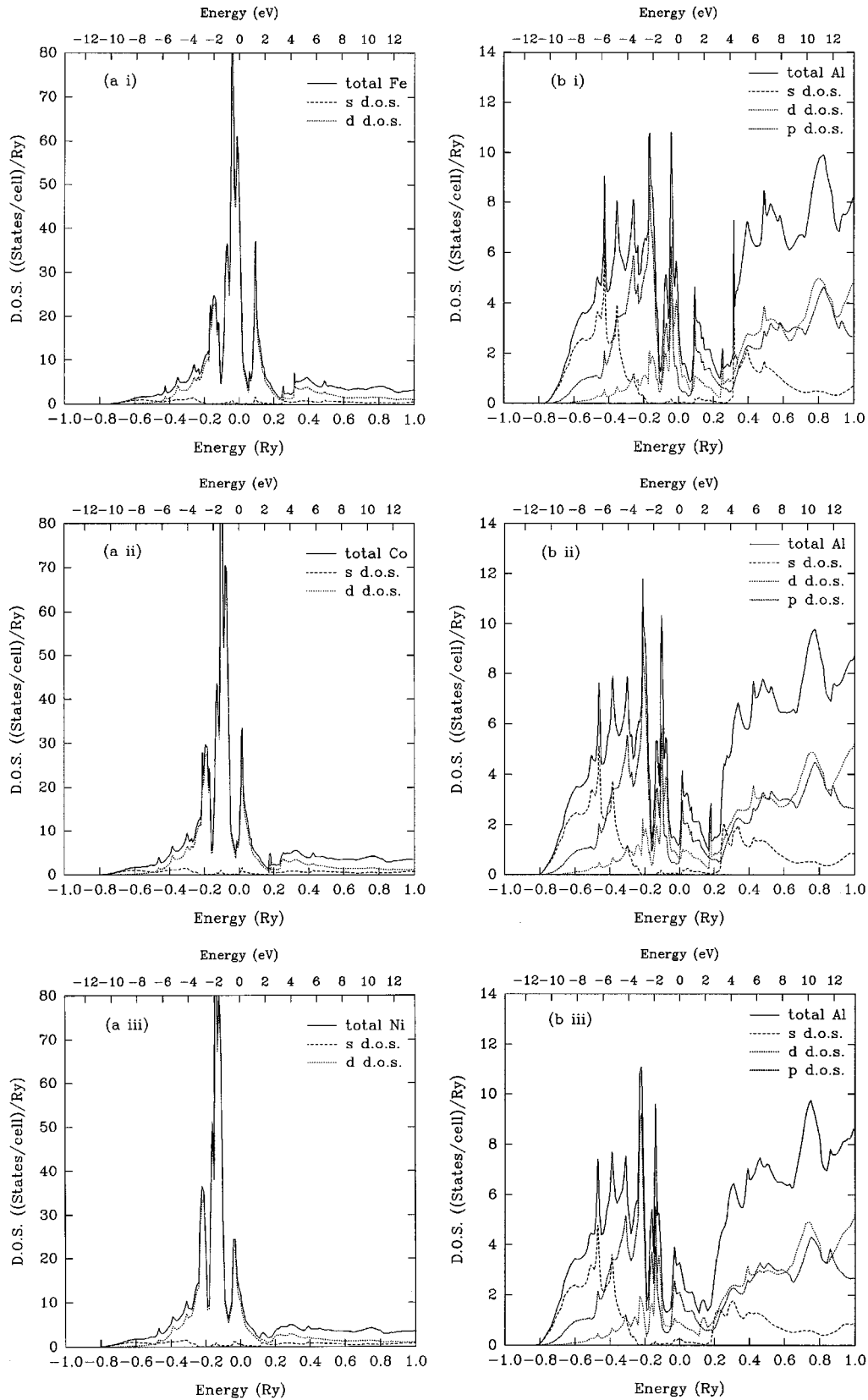


FIG. 5. Density of states in the transition metal aluminides: (a) transition-metal sites in FeAl (i), CoAl (ii), and NiAl (iii) (total DOS and *s* and *d* decomposed).  $E_F$  set to zero. (b) Al sites in FeAl (i), CoAl (ii), and NiAl (iii) (total DOS, *s*, *p*, and *d* decomposed).

important redistribution of the DOS is prevented. Such an effect has also been pointed out by Stern and Rehr.<sup>31</sup> This effect would be less important in early transition-metal aluminides such as TiAl and within our series possibly in FeAl.

However, the agreement between our calculations and experiment for FeAl suggests that even for Fe in FeAl the *d* bands successfully screen the core hole. It is also interesting to point out that the DOS calculated with exchange and cor-

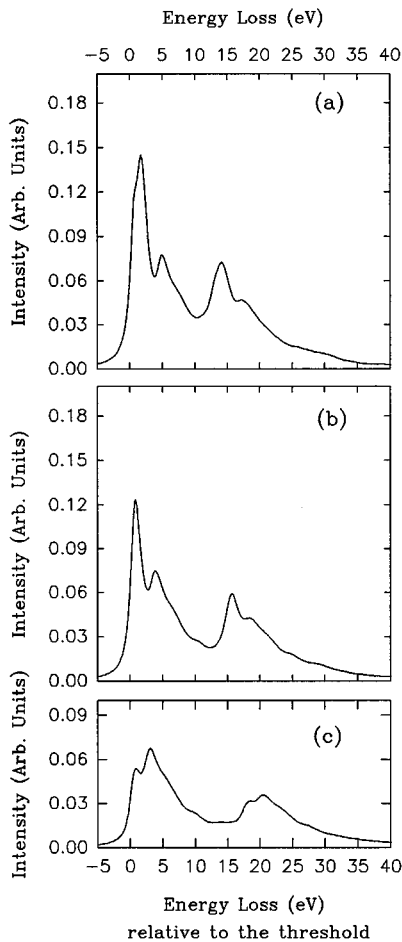


FIG. 6. Calculated energy-loss spectra ( $L_{2,3}$  edges) in the transition-metal aluminides: (a) Fe, (b) Co, and (c) Ni  $L_{2,3}$  edges in FeAl, CoAl, NiAl, respectively (without continuum). The intensity units are equal in the three spectra.

relation energies within the LDA succeed in reproducing the spectral features. Slight discrepancies at higher energy ( $\geq 10$  eV above  $E_F$ ) and the inability to reproduce the continuum are not unexpected considering that we are using a linear method to calculate the DOS.

Because of the agreement between the spectroscopy results and the calculations, and the qualitative understanding of the spectral features we can gain from the DOS, we can express a high degree of confidence in the calculated DOS and in particular the position of  $E_F$ , which affects considerably the relative peak positions in the spectra. We can thus retrieve important information related to the electronic structure and bonding character of these TM aluminides. Directly from the experiments, the decrease in intensity of the TM white lines with respect to the pure metals indicates important changes in the  $d$  bands (see note below concerning the  $d$  charge determination). Apart from the reduction in edge intensity, this conclusion is confirmed in NiAl by the comparison of the experimental near-edge structure (Fig. 1) with the calculated spectrum (Fig. 6) arising from the DOS in which the  $d$  bands are nearly (but not completely) full. Similar behavior is observed in CoAl where the edge intensity decreases (with respect to pure Co) and the fine structure (the stronger peak at the threshold) indicates more empty  $d$  states than in NiAl. The relative position of  $E_F$  and the difference

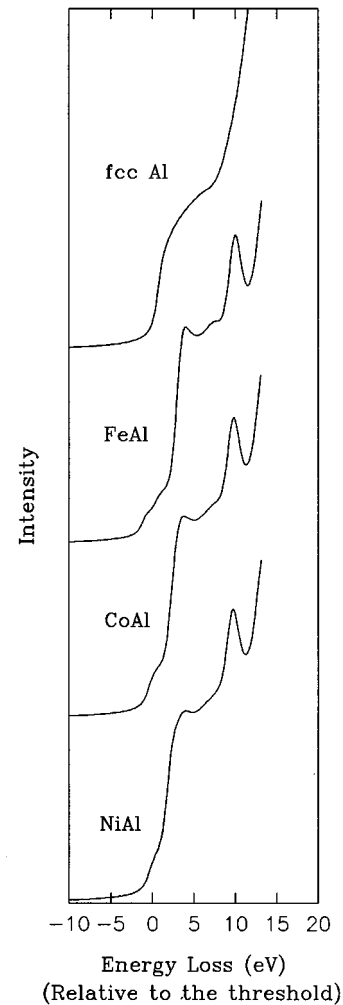


FIG. 7. Calculated Al  $L_{2,3}$  edges in the transition-metal aluminides: FeAl, CoAl, NiAl. The first 15 eV from the threshold are displayed. The spectra are shifted on the intensity scale.

in band filling is well demonstrated by the movement of the shoulder (as pointed by arrows in Fig. 1) in the Co and Ni  $L_3$  white lines. Relative to this shoulder, the first peak of the white line and thus of  $E_F$  (if we assume this peak as a reference point in the band) in CoAl moves by 0.9 eV as compared with the NiAl Ni  $L_3$  white line. This value agrees reasonably well with the shift of the Fermi level of CoAl with respect to NiAl given by the calculations presented above (about 0.08 Ry or 1.0 eV) and differs from the rigid band values. Thus the different degree of  $d$  occupancy in the three alloys is demonstrated by the different peak heights and by their relative intensity of the calculated white lines. Almost full or full  $d$  bands have been suggested by Fuggle *et al.*<sup>6</sup> and Kowalczyk *et al.*<sup>32</sup> to explain valence-band spectroscopy measurements and this effect is clearly demonstrated here from our local unoccupied band analysis. Filled  $d$  bands have also been indirectly proposed from measurements of electronic specific heat<sup>28</sup> and used to model the large heat of formation.<sup>33</sup>

At the Al sites, spectra and calculations show that, in comparison to pure Al, there are extra  $p$ -character empty states (from the Al  $K$  edge), this effect being stronger in FeAl and CoAl. A detailed decomposition of the calculated spectra into their respective  $s$  and  $d$  components is necessary

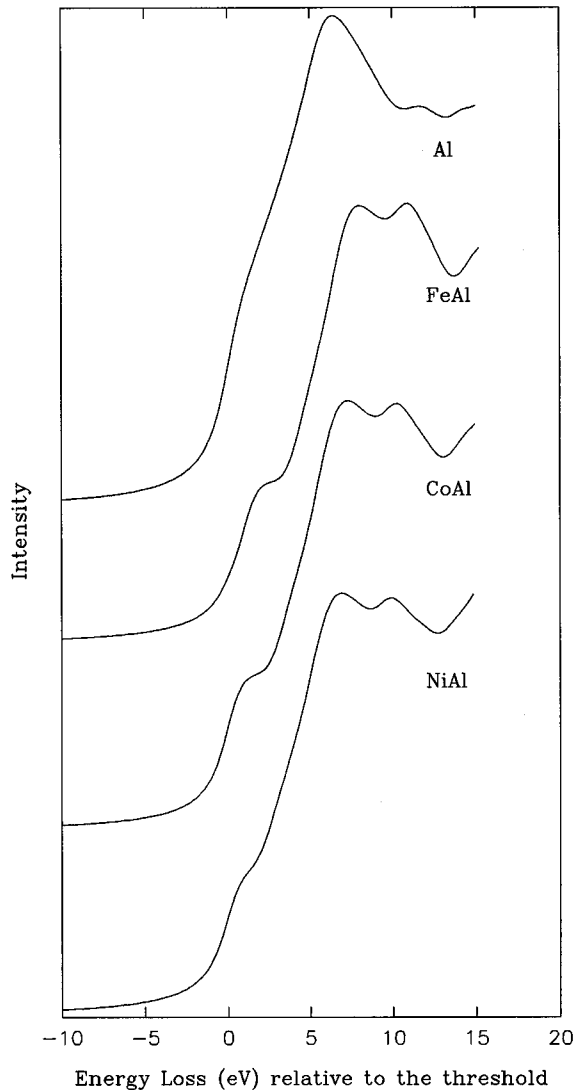


FIG. 8. Calculated Al  $K$  edges in the transition-metal aluminides: FeAl, CoAl, NiAl. The first 15 eV from the threshold are displayed. The spectra are shifted on the intensity scale.

to associate experimental spectral features of the Al  $L$  edges of specific bands. The individual  $s$  and  $d$  components are obtained by artificially setting the matrix elements ( $M$ ) to zero for the appropriate  $L \rightarrow L \pm 1$  transition:  $M^{p \rightarrow d} = 0$  and  $M^{p \rightarrow s} = 0$  to obtain the  $s$  and  $d$  components, respectively. This decomposition (illustrated for FeAl in Fig. 9) indicates that the intensity at the onset arises essentially from the  $d$  component of the DOS while the sharp feature at about 5 eV from the threshold is due to the strong  $s$  character reappearing in the DOS. We note in fact from the DOS that the  $s$  character in the occupied states is strongly suppressed in the energy range  $E = -0.2$  Ry ( $-2.7$  eV) to  $E_F$  due to the introduction of  $d$  character in the same energy range. Strong free-electron  $s$  character is observed at the bottom of the valence band where the amplitude is most important at the Al sites. A displacement of the  $s$  states to lower energy, arising from the interaction of the TM  $d$  states, has been noted by Fuggle *et al.*<sup>6</sup> in soft x-ray emission spectra of noble-metal–Al alloys and is well demonstrated in our calculations, while our experiments indicate also that a similar displacement at higher energy (above  $E_F$ ) occurs. This effect

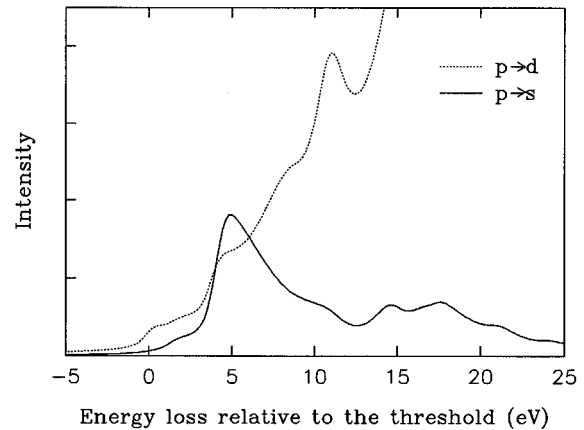


FIG. 9. Al  $L_{2,3}$  edge in FeAl and the decomposed contributions of  $s$  and  $d$  states to the final spectrum. Each contribution is weighted by the appropriate matrix element.

would imply that the free-electron character is pushed to lower energy and thus away from  $E_F$  in these alloys. The effect is therefore more important in NiAl than in FeAl as  $E_F$  is higher in the DOS of the former aluminide with respect to the band center and thus the occupied  $s$  band is deeper.

The angular momentum resolved and site decomposed DOS thus indicates Al  $p$ –TM  $d$  hybridization, which is experimentally supported by the increase of Al  $K$ -edge intensity thresholds. Such hybridization represents the introduction of covalent character in the bond (necessarily directional) and would inevitably contribute to the observed filling of the TM  $d$  bands. We should also point out that the Al  $d$  DOS bears some resemblance to the TM  $d$  DOS and thus we cannot exclude the possibility that the Al  $d$  DOS arises from the tails of the “localized”  $d$  orbitals of the TM atoms. Such a feature is not an artifact of the muffin-tin approach and would imply strong hybridization leading to common electronic states between the Ni and Al sites. This strong interaction could therefore be at the origin of the sharp threshold at the Al edges.

From the spectral variations there is thus clear evidence to suggest that the TM  $d$ -band filling arises from hybridization with the  $p$  valence electrons and some transfer from the less tightly bound electrons from Al, as initially proposed by Hackenbrach and Kübler<sup>28</sup> and Pasturel, Hichter, and Cyriot-Lackmann<sup>33</sup> in order to explain the large heat of formation based on the intensity variations in soft x-ray emission data of Wenger, Bürri, and Steinemann.<sup>4</sup> We note, however, that some of the intensity of the emission spectra in the literature might have arisen from the tails of the TM  $d$  bands as indicated in our DOS. By introducing this  $d$  character, the x-ray emission spectra presented by Fuggle *et al.*<sup>6</sup> and Kapoor *et al.*<sup>5</sup> can be clearly explained, in particular the residual intensity down to 4 eV below  $E_F$ , which could not be modeled solely by the  $s$  component of the DOS. It is therefore likely that the data by Wenger, Bürri, and Steinemann<sup>4</sup> might have been affected in a similar manner. Although it can be computationally ambiguous to determine charge transfer<sup>3,34,35</sup> both x-ray emission and our EELS data<sup>36</sup> indicate that local charge neutrality cannot be assumed in calculations: thus self-consistent computational methods should be used as done in this work. For example, charge transfer is concluded, although qualitatively, in the work of Zou and Fu<sup>2</sup> using FLAPW, in the work of Moruzzi, Williams, and Marcus<sup>37</sup> and Hackenbrach and Kübler.<sup>28</sup> As our analysis

used the LMTO-ASA technique, for which integrated charges depend on the muffin-tin sphere volume with a radius intrinsically related to the unit-cell volume, such an argument cannot be addressed further in this paper as the charges within the sphere in various structures (fcc Fe, Co, Ni, and Al) can be compared only with caution with charges in the alloys. We note, however, that within the spheres used in our calculations, the integrated  $d$  electron charge at the Ni sites increases from 8.55 to 8.66 electrons in going from Ni to NiAl. We also point out that our spectra and calculations imply that, despite the strong hybridization and interaction with the Al  $sp$  electrons, some unoccupied  $d$  character is still present at the TM sites in NiAl and thus the simple rule that Ni is in a  $d^{10}s^0$  configuration as derived from the Hume-Rothery treatment does not describe accurately the electronic structure in this system, hence  $d$  electrons indeed contribute to the bonding.

Finally we address some of the consequences resulting from the DOS and experiments. Concerning the macroscopic properties of the materials, from the DOS we have noted that the bandwidth is different for the three alloys. We would in fact expect different band broadening terms in the heat of formation and cohesive energy due to the fact that TM atoms have to be pulled further apart (relative to their atomic size) by the insertion of the Al atoms into Ni than into Fe and thus the band broadening term in the stability of the lattice is reduced (the bandwidth is inversely proportional to the fifth power of atomic separation<sup>38</sup>). We also note that the lattice parameter decreases from FeAl to CoAl while it increases from CoAl to NiAl in agreement with the fact that we are starting to fill some antibonding states in NiAl.

The differences in band filling also induce differences in properties as the density of states and the electron density distributions at the Fermi level will be greatly different in the three systems. In FeAl,  $E_F$  will be in the bonding states whereas in NiAl these states will be well below  $E_F$ . A high DOS at the Fermi level is generally associated with lower phase stability<sup>39</sup> and thus from our experiments and calculations we would expect a lower stability for FeAl than NiAl. In fact, FeAl, despite being ordered up to its melting point (as CoAl and NiAl), exhibits a higher degree of disorder than NiAl (Refs. 40 and 41) and our electron diffraction data exhibit weak diffuse scattering, indicating small atomic displacements possibly induced by the vacancies and antisite defects. This diffuse intensity is not observed in CoAl and is much weaker in NiAl. A detailed discussion of these effects is beyond the scope of the present paper and will be reported later. In terms of differences in band filling of our alloy series, Freeman *et al.*<sup>29</sup> have demonstrated that charge density maps of electrons near the Fermi energy can be greatly different in similar structures (RuAl and NiAl), which have different band fillings and thus the introduction of defects

and strain under deformation will affect the bond differently.<sup>42</sup> Therefore, contrary to the conclusions of Schultz and Davenport<sup>1</sup> who have analyzed the total valence charge in the systems, analysis of the density distribution at  $E_F$  will be clearly different in the three systems as indicated from our spectra and DOS. The materials will therefore respond differently to defect propagation and thus will exhibit different mechanical properties. A detailed analysis is in progress.

## V. CONCLUSIONS

We have noted a remarkable agreement between experiments and theory. We conclude that in the alloys studied, exchange and correlation effects can be considered within the LDA to explain the spectra with sufficient accuracy. We attribute the agreement of calculated and experimental spectra to the fact that the TM  $d$  bands are almost full, successfully screen the core hole, and thus prevent major redistributions of the unoccupied DOS in the transition metal.

From the analysis of the Al  $L_{2,3}$  and  $K$  edges we note that there are significant redistributions of the unoccupied states as compared with pure Al. Important changes are also observed in the TM  $L_{2,3}$  edges in comparison with the pure elements. These changes are consistent with the interaction of the TM  $d$  band by hybridization with the Al  $p$  electrons. Significant changes in the  $s$  character band are also observed as demonstrated from our spectra and calculations and arise from the introduction of TM  $d$  character at the Al sites. This is clear evidence that covalent character is introduced in the bond.

Variations in occupancy and DOS at  $E_F$  from experiments and calculations indicate that, although unoccupied states are probed, the method is highly sensitive to the electronic structure variations and also that these changes are consistent with variations in macroscopic properties. From spectra we have demonstrated that we can deduce changes in  $E_F$  in the DOS in this series and these agree with calculated values. Although the potential of EELS in high spatial resolution applications is enormous as demonstrated from our bulk analyses, it is clear that consistent interpretation of the data can only be achieved in conjunction with detailed calculations. Building on the success of our methodology, work is in progress to study changes observed at interfaces and in off-stoichiometric materials in terms of the defect structure and the bonding.

## ACKNOWLEDGMENTS

We acknowledge financial support from EPSRC through a ROPA grant. G.A.B. is grateful to Darwin College and NSERC (Canada) for financial support.

<sup>1</sup>P. A. Schultz and J. W. Davenport, *J. Alloys Compounds* **197**, 229 (1993).

<sup>2</sup>J. Zou and C. L. Fu, *Phys. Rev. B* **51**, 2115 (1995).

<sup>3</sup>C. D. Gelatt, Jr., A. R. Williams, and V. L. Moruzzi, *Phys. Rev. B* **27**, 2005 (1983).

<sup>4</sup>A. Wenger, G. Bürri, and S. Steinemann, *Solid State Commun.* **9**, 1125 (1971).

<sup>5</sup>Q. S. Kapoor, L. M. Watson, D. Hart, and D. J. Fabian, *Solid State Commun.* **11**, 503 (1972).

<sup>6</sup>J. C. Fuggle, F. U. Hillebrecht, R. Zeller, Z. Zolnierok, P. A.

- Bennet, and Ch. Freiburg, *Phys. Rev. B* **27**, 2145 (1982).
- <sup>7</sup>X. Weng, P. Rez, and P. E. Batson, *Solid State Commun.* **74**, 1013 (1990).
- <sup>8</sup>P. E. Batson, *Nature* **366**, 727 (1993).
- <sup>9</sup>D. M. Nicholson, G. M. Stocks, W. M. Temmerman, P. Sterne, and D. G. Pettifor, in *High Temperature Ordered Intermetallic Alloys III*, edited by C. T. Liu *et al.*, MRS Symposia Proceedings No. 133 (Materials Research Society, Pittsburgh, 1989), p. 17.
- <sup>10</sup>A. Barbieri, B. L. Gyorffy, M. Sluiter, P. E. A. Turchi, Z. Szotek, and W. M. Temmerman, in *Kinetics of Ordering and Transformations in Metals*, edited by Haydn Chen and Vijay K. Vasude (Minerals, Metals and Materials Society, Warrendale, 1992), p. 101.
- <sup>11</sup>D. Nguyen Mahn, A. Bratkovsky, and D. G. Pettifor, *Philos. Trans. R. Soc. London Sec. A* **351**, 529 (1995).
- <sup>12</sup>A. Messiah, *Quantum Mechanics* (North-Holland, Amsterdam, 1958).
- <sup>13</sup>D. D. Vvedensky, in *Unoccupied Electronic States: Fundamentals of XANES, EELS, IPS and BIS*, edited by J. C. Fuggle and J. E. Inglesfield, Topics in Applied Physics Vol. 69 (Springer, Berlin, 1992).
- <sup>14</sup>D. H. Pearson, C. C. Ahn, and B. Fultz, *Phys. Rev. B* **47**, 8471 (1993).
- <sup>15</sup>H. L. Skriver, *The LMTO Method* (Springer-Verlag, Berlin, 1984).
- <sup>16</sup>O. K. Andersen, *Phys. Rev. B* **12**, 3060 (1975).
- <sup>17</sup>W. M. Temmerman, P. A. Sterne, G.-Y. Guo, and Z. Szotek, *Mol. Sim.* **4**, 153 (1989).
- <sup>18</sup>L. von Barth and J. Hedin, *J. Phys. C* **5**, 1629 (1972).
- <sup>19</sup>B. Poummellec, P. J. Durham, and G. Y. Guo, *J. Phys. Condens. Matter* **3**, 8195 (1991).
- <sup>20</sup>J. Zaanen, G. A. Sawatzky, J. Fink, W. Speier, and J. C. Fuggle, *Phys. Rev. B* **32**, 4905 (1985).
- <sup>21</sup>J. Fink, Th. Muller-Heinzerling, B. Scheerer, W. Speier, F. U. Hillebrecht, J. C. Fuggle, J. Zaanen, and G. A. Sawatzky, *Phys. Rev. B* **32**, 4889 (1985).
- <sup>22</sup>C. B. Boothroyd, K. Sato, and K. Yamada, in *Proceedings of the XII International Conference for Electron Microscopy*, edited by L. D. Peachey and D. B. Williams (San Francisco Press, San Francisco, 1990), Vol. 2, p. 80.
- <sup>23</sup>R. F. Egerton, *EELS in the Electron Microscope* (Plenum, New York, 1986).
- <sup>24</sup>R. D. Leapman, L. A. Grunes, and P. L. Fejes, *Phys. Rev. B* **26**, 614 (1982).
- <sup>25</sup>D. J. Singh, in *Intermetallic Compounds: Principles and Practice, Vol. 1: Principles*, edited by J. H. Westbrook and R. L. Fleisher (Wiley, New York, 1994), pp. 127–147.
- <sup>26</sup>D. J. Singh, *Phys. Rev. B* **46**, 14 392 (1992).
- <sup>27</sup>D. G. Pettifor, in *Electron Theory and Alloy Design*, edited by D. G. Pettifor and A. H. Cottrell (The Institute of Materials, London, 1992).
- <sup>28</sup>D. Hackenbracht and J. Kübler, *J. Phys. F* **10**, 427 (1980).
- <sup>29</sup>A. J. Freeman, T. Hong, W. Lin, and J.-H. Xu, *J. Mater. Res.* **7**, 592 (1992).
- <sup>30</sup>J. Stöhr, *NEXAFS Spectroscopy* (Springer-Verlag, Berlin, 1992).
- <sup>31</sup>E. A. Stern and J. J. Rehr, *Phys. Rev. B* **27**, 3351 (1983).
- <sup>32</sup>S. P. Kowalczyk, G. Apai, G. Kaindl, F. R. McFeely, L. Ley, and D. A. Shirley, *Solid State Commun.* **25**, 847 (1978).
- <sup>33</sup>A. Pasturel, P. Hichter, and F. Cyriot-Lackmann, *J. Less-Common Met.* **86**, 181 (1982).
- <sup>34</sup>R. E. Watson and L. H. Bennett, in *Charge Transfer/Electronic Structure of Alloys*, edited by L. H. Bennett and R. H. Willens (The Institute of Metals, New York, 1974).
- <sup>35</sup>D. J. Gonzalez and J. A. Alonso, *J. Phys. (Paris)* **44**, 229 (1983).
- <sup>36</sup>Although it is clear from the spectra that more empty states are situated at the Al sites in the alloy than in pure Al and less empty states at the TM sites than in the pure elements (see Figs. 1 and 2 for NiAl and Ni), the intensities in the EEL spectra are weighted by the matrix elements and thus do not give a direct representation of the charge within the atomic sphere used in the calculations.
- <sup>37</sup>V. L. Moruzzi, A. R. Williams, and P. M. Marcus, in *Charge Transfer/Electronic Structure of Alloys* (Ref. 34).
- <sup>38</sup>V. Heine, *Phys. Rev.* **153**, 673 (1967).
- <sup>39</sup>Shiyong Pei, T. B. Massalsky, W. M. Temmerman, P. A. Sterne, and G. M. Stocks, *Phys. Rev. B* **39**, 5767 (1989).
- <sup>40</sup>J. M. Koch and C. Koenig, *Philos. Mag. B* **55**, 359 (1987).
- <sup>41</sup>C. L. Fu, Y.-Y. Ye, M. H. Yoo, and K. M. Ho, *Phys. Rev. B* **48**, 6712 (1993).
- <sup>42</sup>C. Woodward, J. M. MacLaren, and S. C. Rao, in *High Temperature Ordered Intermetallic Alloys IV*, edited by L. Johnson, D. P. Pope, and J. O. Stiegler, MRS Symposia Proceedings No. 213 (Materials Research Society, Pittsburgh, 1990), p. 715.